

Adaptive Tracking Control with Application to a Flexible Transmission System

Magnus Nilsson and Bo Egardt

Abstract—This contribution examines the performance of a two-degrees-of-freedom controller with limited adaptive features when applied to a benchmark problem for robust control. A general design procedure is explained and exemplified before simulations are carried out. Simulations indicate that the controller has potential to perform well if applied on the real-world system. However, if the reference-response bandwidth is increased, sudden load changes may lead to unacceptable transients.

I. BACKGROUND AND PURPOSE

Design for traditional adaptive controllers makes little use of *a priori* knowledge about the plant to be controlled. Often, the only *a priori* knowledge assumed for control design is the plant's high-frequency gain, pole excess, order, and that the plant is minimum phase [6]. As a result, much "responsibility" is put on the adaptive controller and this may lead to presumptuous objectives. Also, it is well known from the intense research on robustness for adaptive controllers during the 1980s that traditional adaptive controllers can face serious problems if they are applied without care to real-world systems.

Observations like the above have made some research within adaptive control shift to an approach where the adaptive features are more restricted. This contribution adopts that idea by restricting adaptation to the feedforward part of a two-degrees-of-freedom (2DOF) controller. This is not a novel idea; contributions with this approach can be found scattered throughout the literature. A possible limitation for most such schemes, however, is that they rely on a strictly-positive-real (SPR) condition for the closed-loop system. The authors have recently developed an alternative scheme in [4] where no such SPR condition appears. This paper can be seen as a continued investigation of that scheme within a discrete-time framework.

The purpose of this contribution is to examine how the 2DOF adaptive control scheme developed in [4] performs when applied to the benchmark problem for robust control found in [3]. Less effort is put into theoretical investigation to emphasize pragmatic ideas of the design procedure and show simulation results. The investigated 2DOF control structure may be useful in applications where a precise reference-response is desired but hard to achieve due to uncertainty and nonminimum phase properties.

The control structure from [4] is described briefly in Sec. III before the benchmark problem is described in Sec. IV. A general design procedure is outlined in Sec. V before it is exemplified in Sec. VI when being applied to the benchmark problem. Simulation results are displayed

in Sec. VII before the design procedure is repeated for a case with higher bandwidth in Sec. VIII. Conclusions are mentioned in Sec. IX.

II. NOTATION

The symbol z is used for the forward-shift operator and s is used for the Laplace operator. Arguments are often omitted for convenience (e.g., we write Pr instead of $P(z)r(k)$). Also for convenience, only two significant digits are shown in most formulas and equations. In actual simulations, higher numerical precision was used.

III. CONTROL STRUCTURE

The control scheme developed in [4] is depicted in Fig. 1. The plant $P(s)$ with input $u(t)$ and output $y(t)$ is a linear and time-invariant system controlled by a 2DOF controller consisting of a robust *fixed* feedback controller $C(s)$ and an adaptive feedforward controller $Q(\theta)$. The filter $W_m(s)$ with input $r(t)$ and output $y_m(t)$ acts as a reference model for the closed-loop system. The desired feedforward filter is $Q(s) = W_m(s)/P(s)$, but because the feedforward path is essentially open loop, adaptation is needed when plant knowledge is uncertain. This idea for modest adaptation is natural since a fixed feedback loop can guarantee robustness to instability, while an adaptive feedforward part still allows for perfect model following in a disturbance-free environment.

The original scheme suggests to identify parameters in the plant based on the signals u and y ; this contribution will later present an alternative idea. While the control scheme described in this section was developed for a continuous-time framework, it will here be modified to fit a discrete-time formulation. Adjustments for the estimation algorithm and changes to handle nonminimum phase zeros (that often occur in sampled systems) are discussed in Secs. V and VI.

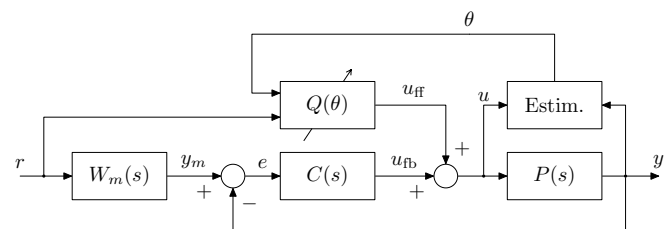


Fig. 1. Block structure of the adaptive controller in [4]

IV. BENCHMARK PROBLEM

The benchmark problem used to exemplify a design procedure and test the performance of the adaptive controller is described in [3]. For the reader's convenience, a brief description of the system and the problem specification now follows.

A schematic picture of the plant is shown in Fig. 2. It is a transmission system consisting of three horizontal pulleys connected by elastic belts. The first pulley is controlled by an electric motor with local feedback, using the reference for the first pulley as its input. The goal is to control the position of the third pulley. A PC is used to control the system. Small weights can be applied to the third pulley to realize different load cases. In the original problem formulation, three different load cases are considered.

The plant for the three modes of operation is described in discrete time as

$$P^{\text{no load}} = \frac{0.28(z + 1.8)}{(z^2 + 0.18z + 0.93)(z^2 - 1.6z + 0.95)} \quad (1)$$

$$P^{\text{half load}} = \frac{0.1(z + 1.8)}{(z^2 - 0.17z + 0.92)(z^2 - 1.8z + 0.97)} \quad (2)$$

$$P^{\text{full load}} = \frac{0.064(z + 1.6)}{(z^2 - 0.24z + 0.92)(z^2 - 1.9z + 0.95)} \quad (3)$$

using the sampling time $T_s = 1/20$ s. These transfer functions will here be assumed to describe the true behaviour of the plant. The plant has a pure time delay of 2 samples. The bode magnitude plots of the three cases are shown in Fig. 3.

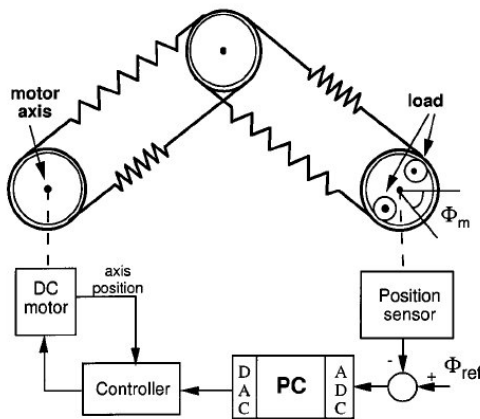


Fig. 2. Schematic picture of the transmission system.

The original specifications in [3] require the controller to be on RST form. This is not taken into consideration. Other than that, the specifications are

- 1) Rise time (0–90% of final value) of less than 1 s for all loads for a reference step response.
- 2) Overshoot less than 10% for a reference step response.
- 3)–8) Disturbance response specifications, not here explained in detail due to space limitations (see [3] for more details).

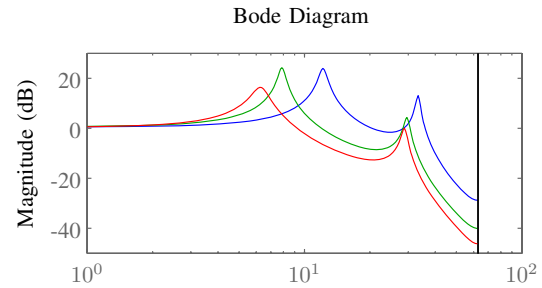


Fig. 3. Bode magnitude plots for the three plant cases. (The higher load, the “lower” amplitude plots.)

With the 2DOF structure used in this paper, the feedback design can focus completely on the disturbance-response specifications 3)–8), while the design of the adaptive feedforward part focuses on specifications 1)–2). We remark that the adaptive controller will not be able to fulfil all specifications at initial stages of adaptation, such as after sudden load changes.

V. DESIGN PROCEDURE

A proposed control-design procedure is now outlined. It assumes that an offline estimate of the plant P with uncertainty is available *a priori* (e.g., as in the benchmark problem considered here) in contrast to assumptions used in many traditional adaptive control design methods.

- 1) Design a robust feedback controller C based on disturbance-response specifications and *a priori* plant knowledge.
- 2) Determine a desired bandwidth from reference to output, and choose thereafter a suitable preliminary reference model W_m .
- 3) Model the plant into the slow part P_{LF} (to be estimated online) and the fast part \widehat{P}_{HF} based on offline estimates and the desired bandwidth.
- 4) Estimate P_{LF} online by using the signals $\widehat{P}_{HF}u_{ff}$ or $\widehat{P}_{HF}u_{ff}$ and y .
- 5) Implement the feedforward controller $u_{ff} = W_m / (\widehat{P}_{LF} \widehat{P}_{HF}) r$.
- 6) If necessary, augment the preliminary reference model to include nonminimum-phase zeros and the time-delay of the plant.¹

VI. DESIGN PROCEDURE APPLIED TO THE BENCHMARK PROBLEM

The steps of the procedure in Sec. V will now be explained in more detail by applying them to the benchmark problem in Sec. IV.

A. Step 1. Feedback design

The feedback may be designed using any appropriate design method, taking only the disturbance-response specifications into consideration. While this step is an important part of the procedure, it is not the main focus of this message.

¹The last two steps of the design procedure may be suitably modified as Sec. VI and VIII will show.

Therefore, we use the feedback part from the controller in [5], which was the winning contribution to the benchmark problem. Its design was based on Quantitative Feedback Theory.

B. Step 2. The reference model

From specifications 1)–2) a preliminary continuous-time reference model that seems suitable is

$$W_m(s) = \frac{\omega^2}{s^2 + 2\zeta\omega s + \omega^2} \quad (4)$$

with $\omega = 3$ rad/s and $\zeta = 0.66$. Discretizing this with zero-order hold and getting rid of time-delays lead to the preliminary reference model

$$W_m(z) = \frac{0.011z(z + 0.94)}{(z^2 - 1.8z + 0.82)}. \quad (5)$$

Its step response can be seen in the upper plot of Fig. 8 (dotted line) and its bode magnitude plot is seen in Fig. 4.

C. Step 3. Divide the plant P into P_{LF} and P_{HF}

The main idea of this frequency separation is to only estimate parameters that are sensitive with respect to the servo performance. As mentioned in Sec. III, the ideal feedforward filter is $Q = W_m/P$. However, if P is estimated with model error, the response from reference to output will not be affected much if this model error is small and only is present for frequencies significantly higher than the bandwidth of W_m . This motivates the separation of P into a low-frequency part P_{LF} that needs to be estimated online and a high-frequency part P_{HF} that only needs an approximate offline estimate.

In Fig. 4 the bode magnitude plot of the reference model is shown together with one plant case. When the plant case is filtered through the reference model, the peak magnitude of the higher resonance becomes approximately -30 dB ≈ 0.03 . Small errors in the estimate of position and magnitude of the higher resonance will therefore not affect the reference-response significantly. A suggested separation of the plant into P_{LF} and P_{HF} is displayed by the dotted line in Fig. 4. This separation is viewed in the complex plane together with a pole-zero map in Fig. 5. From this pole-zero map it is proposed to model P_{LF} with one pair of complex poles, while P_{HF} includes the higher pair of complex poles and the nonminimum-phase zero.

The low-order *a priori* estimates for the three cases (1)–(3) become

$$P_{LF}^{\text{no load}} = \frac{0.37z^2}{(z^2 - 1.6z + 0.95)} \quad (6)$$

$$P_{LF}^{\text{half load}} = \frac{0.16z^2}{(z^2 - 1.8z + 0.97)} \quad (7)$$

$$P_{LF}^{\text{full load}} = \frac{0.1z^2}{(z^2 - 1.9z + 0.95)} \quad (8)$$

while the high-order estimates become

$$P_{HF}^{\text{no load}} = \frac{0.76(z + 1.8)}{z^2(z^2 + 0.18z + 0.93)} \quad (9)$$

$$P_{HF}^{\text{half load}} = \frac{0.63(z + 1.8)}{z^2(z^2 - 0.17z + 0.92)} \quad (10)$$

$$P_{HF}^{\text{full load}} = \frac{0.64(z + 1.6)}{z^2(z^2 - 0.24z + 0.92)}. \quad (11)$$

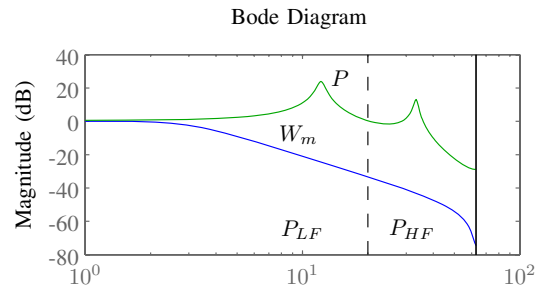


Fig. 4. Bode magnitude plot of preliminary reference model and one of the plant cases. It is sufficient to only estimate the slower resonance online.

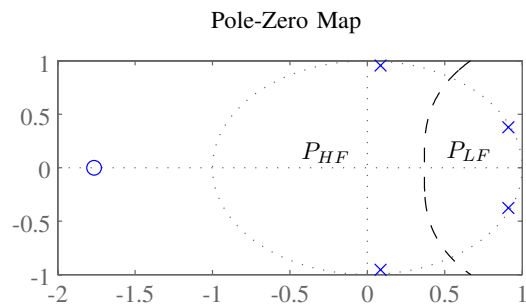


Fig. 5. By inspecting the pole-zero map it is made clear what zeros and poles should be included in P_{LF} and P_{HF} . The dotted line corresponds to the dotted line in Fig. 4 that separates lower and higher frequencies.

D. Step 4. Estimate P_{LF} online

As for any adaptive controller, the choice of estimator structure is important for successful performance of the feedforward controller. Due to the discrete-time formulation, it is natural to apply a simple recursive least squares (RLS) or extended RLS algorithm to estimate the parameters in P_{LF} . It is then important to choose reasonable values for the initial parameter estimates $\theta(0)$, forgetting factor λ , and initial covariance matrix $C(0)$. These values were in simulations chosen as $\lambda = 0.99$, $C(0) = I$, and $\theta(0)$ was chosen as the mean values of the parameter intervals in Table I. Covariance resetting in the RLS algorithm was not used in simulations.

The offline estimate of the faster dynamics was chosen as $\widehat{P}_{HF} = P_{HF}^{\text{half load}}$. Note that all delay in the original plant is modeled in \widehat{P}_{HF} (to be used in the final reference model).

a) *Input signals for the estimator:* The control structure depicted in Fig. 1 suggests that the estimator should estimate a model of the plant based on the input u . Due to the frequency separation in Step 2, this suggests that $\widehat{P}_{HF}u$ should be used. However, this does not work well if a persistent step disturbance acts on the system output. The

reason for this is that the estimator tries to identify P_{LF} based on the model

$$y = P_{LF} \widehat{P}_{HF} u \quad (12)$$

when the output in fact is governed by

$$y = P_{LF} P_{HF} u + v, \quad (13)$$

where v is the disturbance signal. The estimator will thus identify a static gain which is different from the plant's static gain. The performance of the estimator based on (12) is not acceptable since the resulting controller does not fulfil the problem specifications even after adaptation.

One way to modify the estimator that greatly improves control performance under persistent step disturbances is based on the idea that the feedback suppresses the disturbance. Expanding (13) leads to

$$y = P u_{ff} + \underbrace{P u_{fb}}_{\approx 0} + v = \frac{PC + \frac{\widehat{P}_{LF} \widehat{P}_{HF}}{P}}{PC + 1} P u_{ff} + S v \quad (14)$$

where S is the output sensitivity function. If Sv is small—which it should be if the feedback is well designed—it can be seen that an estimator for P_{LF} based on the model

$$y = P_{LF} \widehat{P}_{HF} u_{ff} \quad (15)$$

is reasonable to try. It can be interpreted as a way to estimate and eliminate the disturbance from the measured output.² Such an estimator was used in simulations in Sec. VII and VIII-G.

b) Applying projection based on a priori information: A priori information about parameters may be used in the RLS algorithm to keep the estimate within reasonable bounds. Projection like this can serve as an important guarantee for boundedness of signals in the system. The projection may be implemented by “backtracking” to take a shorter update step in the RLS algorithm when a violation of the bounds is detected. Table I displays the known bounds from (6)–(8) for the parameters in P_{LF} that are to be estimated for a simple RLS algorithm. In simulations it was noted that the convergence rate for the RLS algorithm with this simple way to project parameters could get significantly slowed down when projection became active.

The *a priori* interval for the parameters may depend on what parameterization that is used. For example, the static gain is determined differently in the δ domain compared to the forward-shift domain. A projection scheme based on the δ domain was implemented. It did not, however, lead to any significant differences in signal properties compared to the projection scheme based on the shift domain.

E. Step 5. The feedforward controller

The feedforward controller should implement a delay-free approximate inverse of the true plant; a natural choice is $Q = W_m / (\widehat{P}_{LF} \widehat{P}_{HF})$. Because P_{HF} is nonminimum phase

²Ways to eliminate constant disturbances in traditional adaptive control structures are briefly discussed in [6].

B	A
$[0.1004, 0.3733]z^2$	$z^2 + [-1.8525, -1.6017]z + [0.9484, 0.9722]$

TABLE I

THE LOWER AND UPPER VALUES USED AS A BASIS FOR PARAMETER PROJECTION IN THE RLS ESTIMATOR.

for this example (see Sec. VI-D), the feedforward is instead implemented as a realization of $u_{ff} = W_m / \widehat{P}_{LF} r$, where \widehat{P}_{LF} is time varying. One could let the poles of \widehat{P}_{LF} be included as zeros in the feedforward function, but for this example this does not make much difference to the end result.

F. Step 6. The final reference model

The reason why we include \widehat{P}_{HF} in the reference model is that we simply do not want the feedback to do perform any unnecessary control action. One could as well include \widehat{P}_{HF} in the feedforward controller if it were not for the nonminimum phase zero and time-delay in this example.

The final reference model becomes $W_m \widehat{P}_{HF}$. Its step response can be seen in Fig. 8. Note that this choice of reference model does not give much room for error if the specifications should be met. The control scheme is depicted in Fig. 6

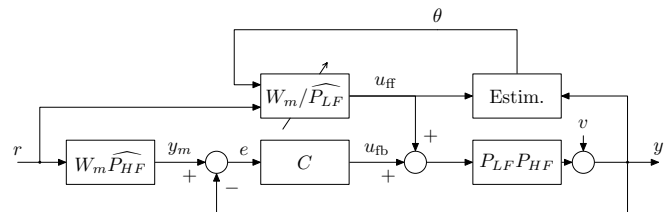


Fig. 6. The final scheme for this particular design.

VII. SIMULATION EXAMPLES

Simulations were carried out in Simulink for the three load cases controlled by the 2DOF controller. The reference was a square wave that changed value between 0 and 1 every 10 s. At $t = 50$ s, a unit output step-disturbance was added to the system and remained constant throughout the simulation. The estimator was based on (15). The output was subject to band-limited white noise with noise power $3 \cdot 10^{-6}$. The simulation started with the full-load case, and then switched to the half-load and no-load cases at $t = 100$ s and $t = 200$ s respectively.

Fig. 7 shows the output for the whole time period. It can be seen that the transients at load changes are reasonably small. Fig. 8 shows step responses at $t = 40$ s, $t = 140$ s, and $t = 240$ s. The output follows the reference model closely and the specifications are fulfilled for steps made at these points in time. A typical input signal at a step change is shown in Fig. 9.

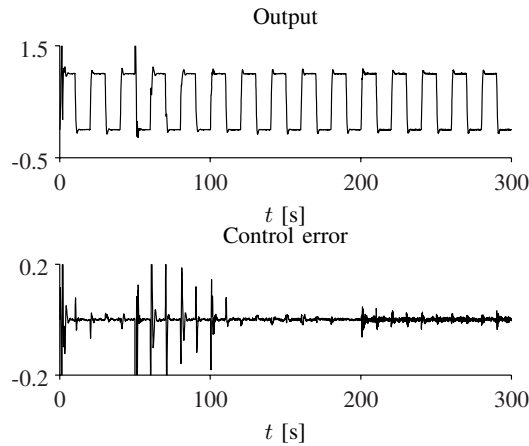


Fig. 7. Output (upper) and control error (lower plot) throughout the simulation. The controller has trouble keeping the error small for a few periods after the step disturbance is introduced. Note that the control error is larger than what the plot can display at some periods of time.

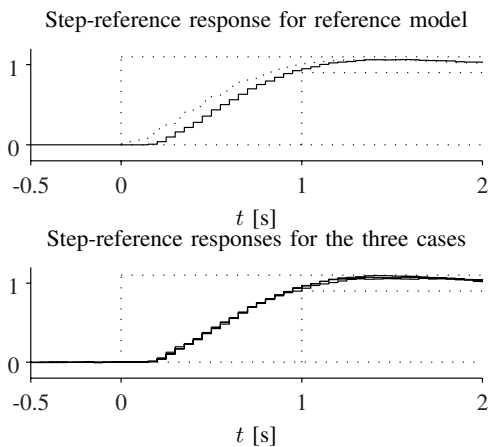


Fig. 8. The upper plot shows step responses for the preliminary reference model W_m (dotted) and final reference model $\widehat{P}_{HF}W_m$ (solid). The only significant difference between the responses is a time delay of two samples. The lower plot shows step responses from $t = 40$ s, $t = 140$ s, and $t = 240$ s for the three loads for the examined structure. The specifications for rise time and overshoot are outlined by dotted lines. Compare this figure with Fig. 7.

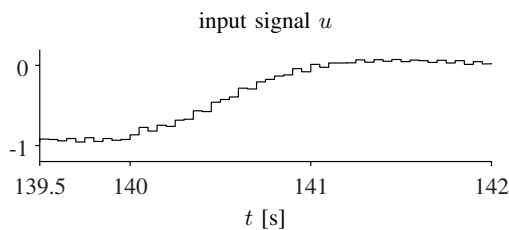


Fig. 9. The input for a typical step change. The reason why the input is so noisy is because the additive output noise is amplified much by the feedback controller taken from [5]. The level of the input starts near -1 since the output step disturbance is acting on the system for this time period.

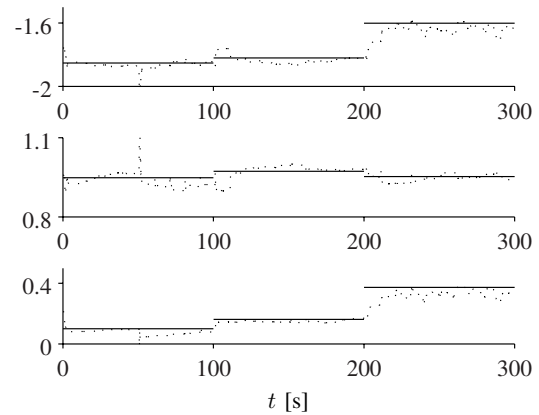


Fig. 10. Parameter estimates and their true values throughout the simulation. The parameters were in this case allowed much freedom to reward parameter convergence; see Sec. VI-D.0.b.

VIII. CONTROLLER REDESIGN FOR HIGHER BANDWIDTH

Adapting the feedforward part may be of interest in applications where high bandwidth from the reference is desired but hard to achieve by feedback only. Since the plant has a pure time-delay $T_d = 0.1$ s, the rough estimate $\omega_b < 1/T_d$ (see e.g. [1]) gives $\omega_b \approx 10$ rad/s as an upper limit of the highest bandwidth that can be achieved using feedback only. To make things more challenging for the 2DOF control structure, the bandwidth of the reference model was therefore changed to $\omega_b = 10$ rad/s, which corresponds to a rise time of 0.4 s including the time delay. The design procedure will now be repeated for this case.

A. Step 1. Feedback design

The feedback used in simulations is the same as in Sec. VI-A.

B. Step 2. Reference model

A second order model on the same form as (4) with $\omega = 10$ rad/s and $\zeta = 0.66$ translated to discrete time leads to $W_m^{\text{fast}} = \frac{0.099z(z+0.8)}{(z^2-1.3z+0.52)}$. It has a step response corresponding to the dotted line in the upper plot in Fig. 12.

C. Step 3. Divide the plant P into P_{LF} and P_{HF}

The higher peak resonance of $P^{\text{no load}}$ when filtered through the fast reference model W_m^{fast} becomes approximately -10 dB ≈ 0.3 . Therefore, both resonances needs to be modeled in the feedforward path for acceptable performance. Modeling of the nonminimum phase zero could be omitted but is included for the purpose of showing that the final reference model can include time-varying elements. This means that $\widehat{P}_{HF} = 1/z^2$ for this case.

D. Step 4. Estimate P_{LF} online

This step is similar to the previous case, only more parameters needs to be estimated for the faster case. Projection can be used based on information from (1)–(3).

E. Step 5. Feedforward controller

The online estimate is divided into $\widehat{P}_{LF} = \widehat{B}_+ / \widehat{A}$, where \widehat{B}_+ denotes the non-Hurwitz denominator. The feedforward function is thereafter implemented as a realization of $u_{ff} = W_m^{fast} \widehat{A} / \widehat{b}_{+0} r$, where \widehat{b}_{+0} is the static coefficient of \widehat{B}_+ .

F. Step 6. Final reference model.

The final reference model becomes $\widehat{B}_+ W_m / \widehat{b}_{+0} \widehat{P}_{HF}$. Dividing by \widehat{b}_{+0} is necessary to maintain unity static gain for the reference model. Since projection is used, the location of the estimated nonminimum-phase zero is guaranteed to stay within an interval that does not affect the reference-response significantly. The step response of the final reference model is seen in Fig. 12.

G. Simulation results

The same simulation setup as for the previous case in Sec. VII was used. Again, the estimator was based on the model (15) to achieve better performance under disturbances. The simulated output signal is shown in Fig. 11. It should be noted that the scheme now exhibits transients at load changes that the real-world system may not be able to handle. However, after only a few steps the controller adapts to a nice response very close to the reference output, as indicated in Fig. 12. The input signal during a step change is seen in Fig. 13.

When a high bandwidth is desired and significant time delays are present, there may not be any way to handle sudden load changes well. This can be understood by realizing that after a sudden load change, it will take time before this can be noted at the output. During this time delay the feedforward controller may induce large transients in the system. In fact, when a constant feedforward controller adjusted for one of the plant cases was used in simulations, the error at other load cases was in the same order of magnitude as transient errors experienced by the adaptive controller.

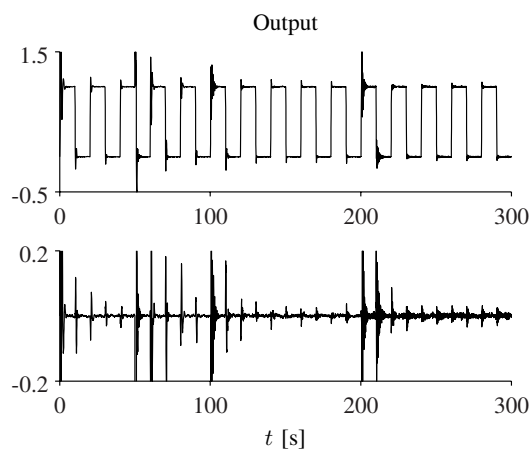


Fig. 11. Output signal (upper plot) and control error (lower plot) for the system with higher bandwidth. Note that the control error is larger than the plot displays at some periods of time.

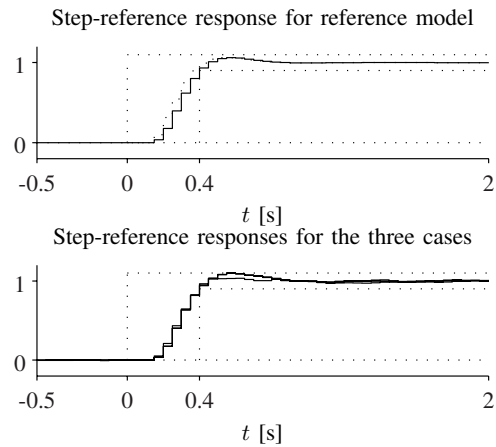


Fig. 12. Step responses for the reference model (upper plot) and the output (lower plot) at $t = 40$ s, $t = 140$ s, and $t = 240$ s. See also Fig. 11.

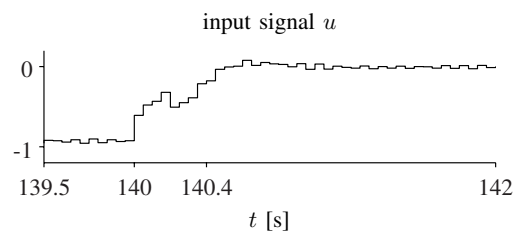


Fig. 13. The input for a typical step change for the high-bandwidth case. Compare with Fig. 9

IX. CONCLUSIONS

A design procedure for adaptive tracking control has been outlined and exemplified. As most adaptive schemes, the controller faces difficulties to handle sudden load changes, but performs well after adaptation. The adaptive controller also performs well under output disturbances when the estimator is based on the feedforward input signal u_{ff} . To try the scheme with a high bandwidth on the real-world system likely requires a more elaborate scheme to handle sudden load changes. Ideas from [2] may be of interest if this would be pursued.

REFERENCES

- [1] Torkel Glad and Lennart Ljung. *Control Theory: Multivariable and Nonlinear Methods*. Taylor & Francis, New York, NY, 2000.
- [2] Alireza Karimi and Ioan Dor Landau. Robust adaptive control of a flexible transmission system using multiple models. *IEEE Transactions on Control Systems Technology*, 8(2):321–331, March 2000.
- [3] I.D. Landau, D. Rey, A. Karami, A. Voda, and A. Franco. A flexible transmission system as a benchmark for robust digital control. *European Journal of Control*, 1(2):77–96, 1995.
- [4] Magnus Nilsson and Bo Egardt. A clarifying analysis of feedback error learning in an LTI framework. *Accepted for publication in the International Journal of Adaptive Control and Signal Processing; published online 6 Feb 2008*, — 2008.
- [5] Mattias Nordin and Per-Olof Gutman. Digital QFT design for the benchmark problem. *European Journal of Control*, 1(2):97–103, 1995.
- [6] Karl Johan ström and Björn Wittenmark. *Adaptive Control*. Addison-Wesley, second edition, 1995.